COPY

NASA Contractor Report 181731
PSI-1011/TR-800

A Laser Spectrometer and Wavemeter for Pulsed Lasers

J.A. McKay, P.M. Laufer, and L.J. Cotnoir

Physical Sciences Inc.
Washington Operations
635 Slaters Lane, #G101
Alexandria, VA 22314

Final Report
Contract NAS1-18243

September 1989

National Aeronautics and
Space Administration

Langley Research Center
Hampton, Virginia 23665-5225

A LASER SPECTROMETER AND WAVEMETER FOR PULSED LASERS

CONTENTS

LIST OF FIGURES

LIST OF TABLES

Page

A LASER SPECTROMETER AND WAVEMETER FOR PULSED LASERS

Introduction

The design, construction, calibration, and evaluation of a pulsed laser wavemeter and spectral analyzer will be described here. This instrument, which we call the Laserscope for its oscilloscope-like display of laser spectral structure, has been delivered to NASA Langley Research Center as a prototype of a laboratory instrument. It will be evident from the following that this prototype does not function as well has had been hoped, as is to be expected from a first model. The description in these pages will summarize the design, construction, and software operation of the Laserscope, with two objectives. First, the prototype delivered will be useful, despite its imperfections, and this report will provide a detailed description of its operation. Second, a full description of the unit, including in particular the origins of its shortcomings, will be invaluable in the development of an improved model.

The heart of the instrument is a Fizeau wedge interferometer, providing high resolution and a linear dispersion of spectral information, ideally suited to linear array photodiode detectors. Even operating alone, with the classic order-number ambiguity of interferometers unresolved, this optical element will provide a fast, detailed indication of the spectral structure of a laser output. If precise wavelength information is also desired -- the "wavemeter" function -- then additional stages must be provided to obtain a wavelength measurement within the order-number uncertainty, i.e. within the free spectral range of the Fizeau wedge interferometer. The Snyder wedge is included to provide this initial wavelength measurement.

Snyder Wedge: Theory of Operation

The spectrometer was built around a cascade of two optical interferometers, both featuring compactness, ruggedness, and single-pulse capability. The first stage of the instrument is a Snyder wedge, an optical device which has seen fairly extensive development [1-11], especially by J.J. Snyder of the National Bureau of Standards. This device has been reported to be capable of wavelength measurement to a few parts in 10^7 for cw lasers, one in 10^6 or better for pulsed lasers.

The sole function of the Snyder wedge in the current instrument is the determination of the wavelength with sufficient accuracy that the order number in the Fizeau wedge can be uniquely determined. Since the Fizeau wedge spacing e_F was 3.5 cm, the order number m_F ($=2e_F/\lambda$) is about $1x10^5$, and a wavelength measurement accuracy of about $5x10^{-6}$ (5 ppm) is sufficient (Figure 1). Because this is a factor 5 poorer than is indicated by other builders of Snyder-wedge interferometers, and an order of magnitude inferior to the accuracy claimed for cw lasers with Snyder wedges, it was thought that this could be achieved without great difficulty. This, as will be evident in the evaluation of the performance of the instrument, was a miscalculation.

The Snyder wedge is a single element which acts as a two-stage optical device. The pair of reflections from the two uncoated faces of the wedge combine to produce a very simple interference pattern, given by

$$I(x) = I_0\{1 + \cos[2\pi(x-x_0)/\Gamma]\} \quad , \tag{1}$$

where I(x) is the intensity along the wedge (perpendicular to the wedge vertex), x_0 is the location of a maximum, and $\Gamma=\lambda/2\tan\alpha_s$, where α_s is the wedge angle. The <u>first pass</u> wavelength measurement involves merely measuring the fringe spacing Γ and using $\lambda=2\Gamma\tan\alpha_s$. Thus the wavelength computation begins with absolutely no *a priori* information on the laser wavelength.

The second-pass wavelength computation uses the Snyder wedge as a classic interferometer. Given an interference maximum at some location x_1 (any of the many fringes along the wedge can be selected), one uses the interference equation,

$$2(e_s + x \tan\alpha_s) = (m_s + 1/2)\lambda \quad , \qquad (2)$$

where e_s is the Snyder wedge spacing at the arbitrary point x=0, and m_s is the order number of the maximum. The term 1/2 accounts for a phase reversal upon reflection at the second wedge face, while no phase reversal occurs at the first-face reflection.

The measurement accuracy required from the first pass for the unique determination of m_s in the second is $\pm 1/2m_s$, or approximately $\pm\lambda/4e_s$. The measurement accuracy of the second pass is

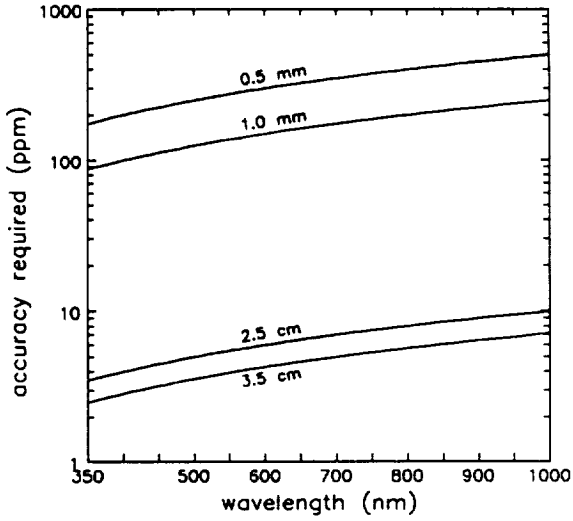

Figure 1. Required wavelength measurement accuracy for unambiguous order number determination, for interferometers of various spacings.

$$\delta\lambda/\lambda = \alpha_s\delta x/e_s, \qquad (3)$$

where δx is the uncertainty in the location of the fringe. (For the moment we will deal only with uncertainties due to instrumental measurement resolution limits, rather than systematic deviations due to calibration uncertainties.)

Initially a Fizeau wedge spacing of 2.5 cm was assumed, a value which was practical and promised to provide the necessary spectral resolution. Then, at 750 nm wavelength, a second-pass Snyder wavelength measurement accuracy of 7.5×10^{-6} is required. Assuming typical Snyder-wedge parameters of e_s=1 mm and α_s=1 mradian, this requirement implies a fringe-location uncertainty δx of less than 7.5 μm, or 0.3 of a 25-μm detector pixel.

As difficult as that might appear, the requirement on the first pass of the Snyder measurement is worse. Again assuming a 1 mm Snyder wedge, the first pass must yield an accuracy of better than 2×10^{-4} (Figure 1). The uncertainty in the first-pass wavelength determination is simply

$$(\delta\lambda/\lambda)_1 = 2\alpha_s\delta\Gamma/\lambda \; . \qquad (4)$$

The fringe spacing Γ must be measured to this accuracy. The 1 mrad angle yields, at 750 nm wavelength, a fringe spacing of 375 μm, and the absolute spacing uncertainty $\delta\Gamma$ must therefore be less than 70 nm, or 0.003 of a 25 μm pixel.

These calculations were generalized in order to obtain a clear picture of the requirements for the Snyder wedge. The first-pass uncertainty, eq. (4), must be less than $1/2m_s$, where $m_s=2e_s/\lambda$, the Snyder-wedge order number. Then the uncertainty in measurement of the fringe spacing must satisfy

$$\alpha_s\delta\Gamma < \lambda^2/8e_s \; . \qquad (5)$$

This is shown in Figure 2, for the entire wavelength range that might be covered by the interferometer. The spacing uncertainty dimension δx is given as $w\delta p$, where w is the width of a pixel and δp is the measurement uncertainty in pixels. Solid lines show the results for a variety of possible Snyder wedge spacings. Broken lines show the maximum allowable fringe spacing uncertainty in pixels for α_s=1 mrad and w=25 μm. Evidently fringe spacing measurements to a few thousandths of a pixel are necessary.

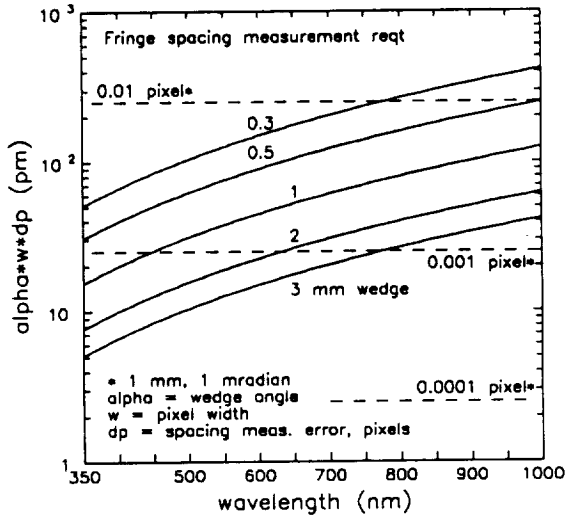

Figure 2. Fringe spacing measurement requirement.

This may exaggerate the difficulty of the first-pass Snyder calculation. One measures not a single fringe pair but a sequence of fringes, limited only by the finite length of the detector, and averages the spacing. The number of fringes n on a detector of length Nw (where N is the number of elements, or pixels, of the detector) is $n=\mathrm{Trunc}(2\alpha_s Nw/\lambda)$, a number typically on the order of 70. ("Trunc" denotes truncation of the real number to an integer.) This total spacing $n\Gamma$ must be measured to the appropriate precision, $\lambda/4e_s$:

$$\delta(n\Gamma) < \lambda Nw/4e_s \ , \tag{6}$$

where the approximation $n\Gamma \approx Nw$ has been employed. Figure 3 and Figure 4 show Eq. (6) evaluated for two candidate detectors, an array of 1024 25 μm elements and an array of 1024 13 μm elements. The first is the device initially intended for use in the wavemeter, while the second is the device in fact selected.

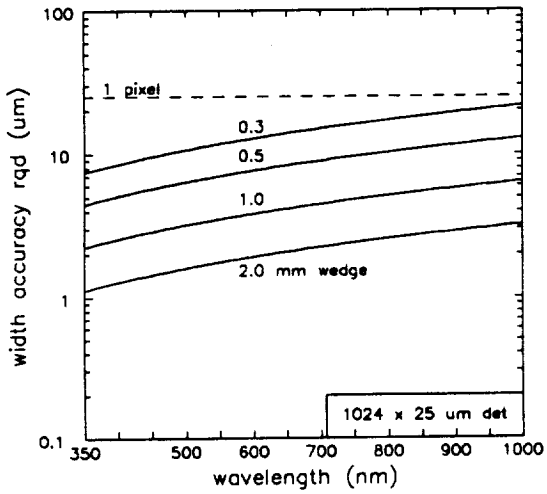

Figure 3. Fringe spacing measurement requirement, 1024 x 25 μm detector.

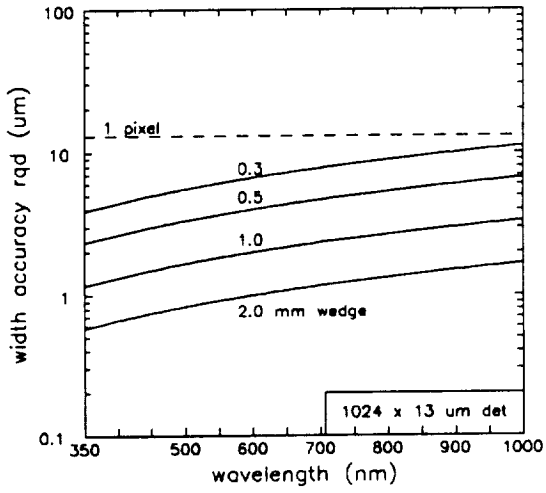

Figure 4. Fringe spacing measurement requirement, 1024 x 13 μm detector.

Evidently the full fringe pattern must be measured to a precision better than a single pixel. At 750 nm wavelength, the pattern length measurement accuracy required for a wedge with 0.5 mm spacing is ±0.4 pixel; with 1.0 mm spacing, the necessary accuracy is ±0.2 pixel.

This exceeds the capability of the apparatus if a simple fringe-measurement analysis is employed. If one simply measures the endpoints as carefully as possible, and uses the intervening elements to obtain a count of fringes, the accuracy of pattern measurement is ±2 pixels. A more sophisticated method is necessary to achieve higher measurement precision. (We note, however, that a very fast system could be devised by using wedges with spacing small enough to function with 2-pixel first-pass accuracy.)

The Snyder Analysis Algorithm -- First-pass Wavelength Determination

The Snyder analysis algorithm [3] is an analysis technique which achieves the necessary higher accuracy, at considerable cost in computation time, though avoiding the evaluation of transcendental functions. The essential principle of this analysis is the convolution of a symmetric, square-wave filter against the fringe pattern, a procedure which yields a zero output when the filter is centered on the sinusoidal pattern. The integral of Eq. (1) against a square-wave function with value -1 for $-b \le x \le 0$ and +1 for $0 \le x \le b$ is

$$I_0 \left[(\Gamma/2\pi) \left\{ \sin 2\pi(b-x_0)/\Gamma - \sin 2\pi(b+x_0)/\Gamma \right\} \right] , \qquad (7)$$

which vanishes if x_0 is an integral multiple of $\Gamma/2$. The converse is that, if a square-wave filter is convolved against a sinusoidal fringe, the integral vanishes if the square wave is positioned with its crossover point located at a node of the sinusoid, either a maximum or a minimum.

Snyder [3] shows that this result is valid even in the case of a modulated sinusoid, as is more characteristic of fringe patterns, and obtains also an optimal value of the filter length 2b, namely 0.742 times the fringe period.

The Snyder technique for fringe analysis consists of the following steps:

(1) The filter length *b* is selected. Initially this uses a guessed value for the fringe spacing.

(2) The integral of the square-wave filter against the fringe pattern is computed, initially for the filter at one extremity of the pattern.

(3) The filter is then translated through the fringe pattern, and the integral evaluated at each pixel. This evaluation is quite efficient, since an evaluation after a single-pixel translation requires only an adjustment of the four pixels affected by the translation, namely the two at the endpoints and the two at the crossover point. Each zero crossing of the integral is recorded.

(4) The result of the convolution is a list of the zero crossings, or nodes, of the pattern. This is the array *nodes[i]* in the computer program. Ideally this is simply a straight line, since the nodes must be equally spaced, with spacing $\Gamma/2$. An average node spacing is obtained, filtering out the noise in the system, by applying a least-squares linear fit to the array nodes[i].

(5) The fringe period obtained from the node spacing is compared with the value used in the filter convolution. If the period obtained from the convolution is significantly different from that assumed for the convolution, the process is repeated, beginning at step (1), now with the improved fringe spacing. Ordinarily only a single repeat is necessary.

(6) The node spacing is used to compute the first-pass Snyder wavelength. This is then used to calculate the order number at the first maximum of the fringe pattern. The location is obtained to high precision, averaging over all the fringe node locations, from the least-squares fit of (4). The fringe location and the order number yield, in the classic manner of interferometers, the wavelength to substantially improved accuracy. This is the second-pass Snyder wavelength and will be the input to the Fizeau-wedge calculation.

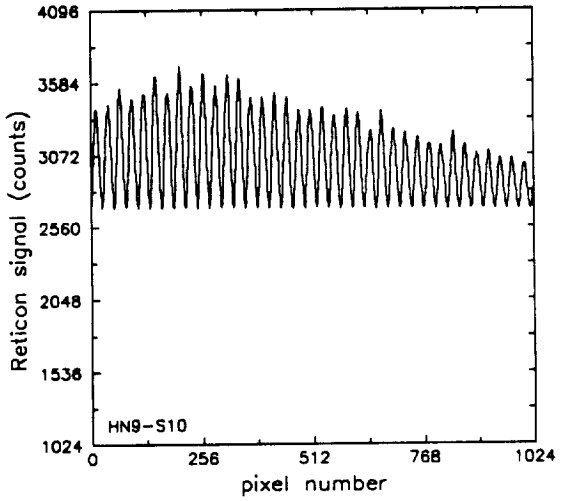

Figure 5. Snyder interference pattern, cw HeNe laser.

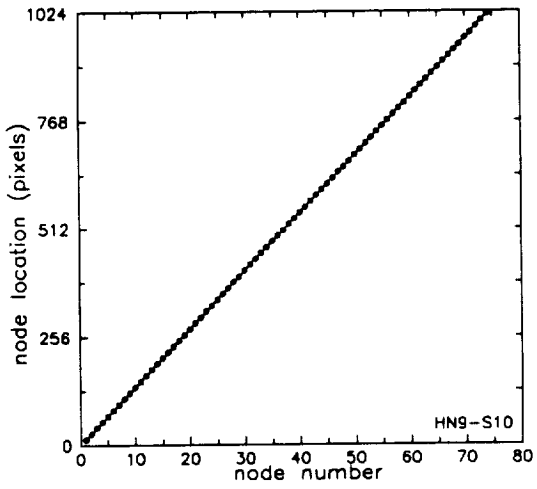

Figure 6. Node location data for the cw laser.

Figure 5 and Figure 6 illustrate the procedure. Figure 5 is a Snyder interference pattern obtained with the PSI/URF Laserscope, with a tunable helium-neon laser (PMS Electro-Optics LSTP-0020), set to 594.1 nm, as the source. The actual fringe period is 27.5 pixels. The first guess at the fringe period is 30 pixels, an arbitrary number which would be correct for a wavelength of about 650 nm. The filter length $2b$ is set to this first-guess period multiplied by 0.742, or 22 pixels. The filter with this initial length is convolved against the fringe pattern to obtain a first list of node locations, each node corresponding to a maximum or a minimum of the fringe pattern. Because of the averaging effect of the 22-pixel-wide filter, modest high-frequency noise on the pattern does not cause spurious nodes to be identified.

The list of nodes is averaged, using a least-squares linear fit, to obtain a node spacing, and hence the fringe spacing. The first pass through the filter yields 27.5077 pixels for the fringe spacing. The corresponding ideal filter width, using the Snyder coefficient, is 20 pixels, rather than 22. This change requires an iteration of the filtering, now with the different filter length. The second iteration yields a very slightly different fringe spacing, 27.5072 pixels.

This small change in fringe spacing leads to an unchanged filter length, so the fringe filter operation is terminated.

Figure 6 shows a set of node-location data from the filter operation on the fringes of Figure 5. The deviation from a straight-line fit is invisible. A clearer indication of the scatter in the node spacings (half the fringe period) is given by Figure 7, a plot of the successive differences in node location. The node spacing, node-to-node, varies by as much as 1.5 pixels from the average.

As Figure 2 showed, it is necessary to measure the fringe spacing (twice the node spacing) to an accuracy of several thousandths of a pixel. The scatter in node spacing indicated by Figure 7 suggests that this will be difficult.

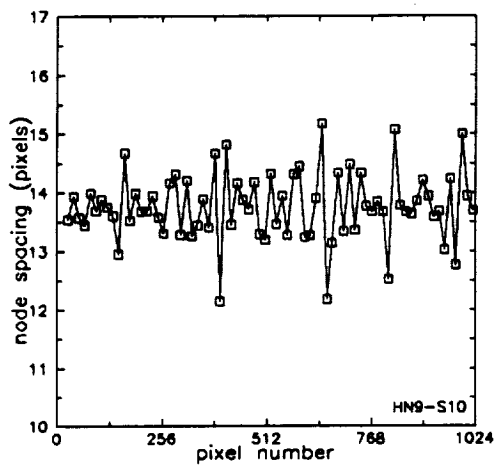

Figure 7. Node location data, cw laser.

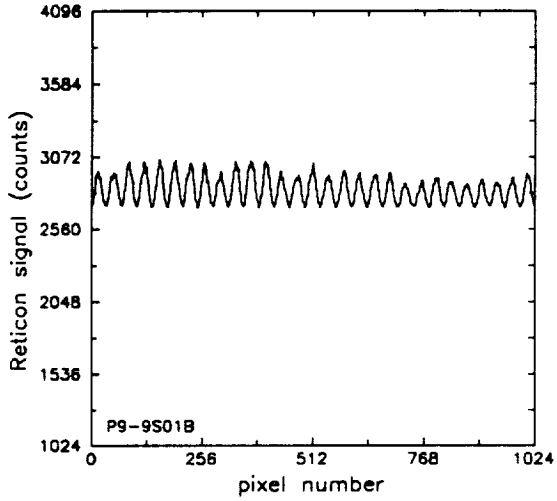

Figure 8. Snyder interference pattern, pulsed dye laser.

Pulsed lasers in general produce fringes inferior to those of cw lasers. Figure 8 is a Snyder wedge fringe pattern, randomly selected, from the Laserscope tests with the University of Maryland Lidar Lab dye laser. The increased level of high-spatial-frequency noise is obvious. Figure 9 shows the node spacing scatter for this pulse; compare Figure 7, drawn to the same scale. The range of variation in the node spacing is about 4.5 pixels, a thousand times larger than the accuracy required from this measurement.

Given these large variations in node spacing, it is somewhat surprising that the interferometer works at all. It should not be surprising, in retrospect, that this portion of the wavelength and spectral analysis turned out to be the weakest link in the system.

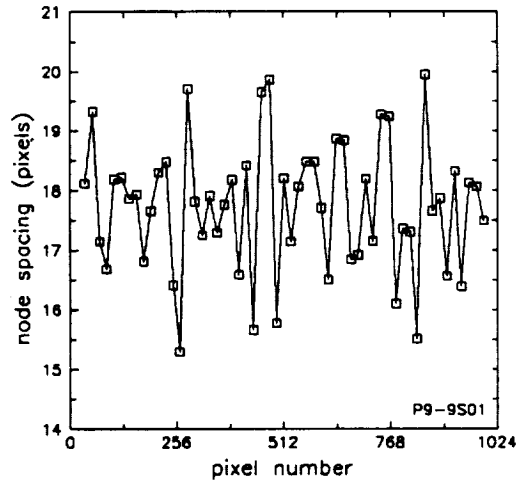

Figure 9. Node spacing data, pulsed dye laser.

Second-pass Wavelength Determination

By the second-pass calculation of the wavelength we mean the relatively straightforward evaluation of wavelength from the location of a fringe, given the wavelength with sufficient accuracy that the order number of that fringe can be specified.

The least-squares fit to the nodes (Figure 6) yields an improved, pattern-averaged evaluation of the node locations. The y-intercept of the linear fit is the location of the "zeroth" node. The polarity

of the first node indicates whether this node is a minimum or a maximum. If it is a minimum, the location is incremented by the node spacing to obtain the location of a maximum. If the location is negative, it is incremented by the fringe spacing to obtain a positive value for the fringe location.

This location is then used in the classic interferometer manner, Eq. (2), to obtain the wavelength to improved accuracy. That is, the order number is calculated as a real value from the fringe location, the wedge spacing at that location, and the approximate (first-pass) wavelength. The order number is rounded to the nearest integer, and the wedge spacing used again to obtain the second-pass wavelength.

The measurement accuracy required from this operation, for the unique determination of the order number m_F in the Fizeau wedge, is $\pm 1/2m_F$, or approximately $\pm\lambda/4e_F$ (Figure 1). The measurement accuracy of the second pass was given by Eq. (3). Then the required accuracy of determination of the fringe location is given by

$$\delta x < (e_S\lambda)/(4e_F\alpha_S) \quad . \tag{7}$$

Figure 10 shows this parameter, as the product $\alpha_S w \delta p$, for several values of Snyder wedge spacing e_S. The results in terms of pixels, for a Snyder wedge with e_S=1 mm and α_S=1 mradian, are also indicated. Evidently a measurement accuracy of a few tenths of a pixel is necessary.

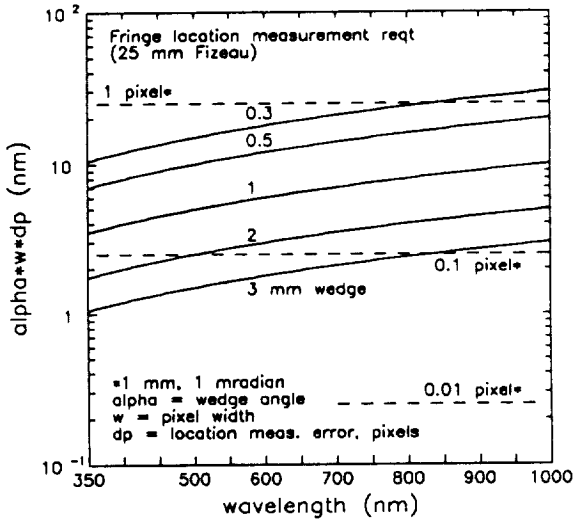

Figure 10. Snyder fringe location measurement requirement.

This is considerably less stringent than the requirement of several thousandths of a pixel imposed on the first-pass Snyder calculation. A natural question is whether a better match might be obtained, perhaps decreasing the wedge angle to spread out the fringes and relax the fringe-spacing specification. An extensive modeling task was undertaken to determine if there might be optimal values of Snyder wedge angle and spacing, yielding less stringent demands on the fringe measurements. This modeling involved developing the Snyder analysis software and applying it to computer-generated fringe patterns, patterns with noise, modulation envelopes, detector nonuniformity, odd-even pixel noise, and analog-digital conversion limitations added to simulate a realistic fringe pattern.

Figure 11 and Figure 12 show some of the simulation results. The points indicate various permutations of the conditions of fringe pattern degradation, e.g. different modulation envelopes. The calculations were performed for a fixed wavelength of 730 nm.

The somewhat surprising result of this modeling was that there are no optimal values of Snyder wedge angle or spacing. Excepting the pathological limit of very small angle or spacing, the resulting system accuracy and perturbation resistance are practically independent of the wedge parameters.

The modeling was done long before the apparatus was built, since of course it was desired to base the prototype design on the modeling results. Figures 11 and 12 suggest that the Snyder wedge should perform practically faultlessly for all the pattern degradations imposed. The error values are well below the level required for the 3.5 cm Fizeau wedge. This is, in fact, a very optimistic conclusion. In practice, the reliability of the Snyder wedge was found to be substantially inferior to the modeling prediction.

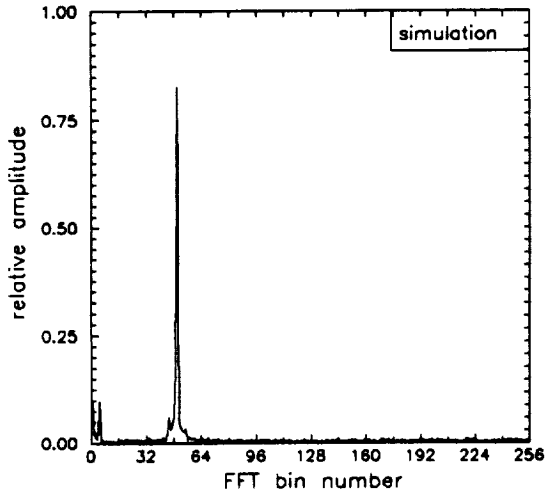

Figure 13. Fourier spectrum of a simulated Snyder wedge interference pattern.

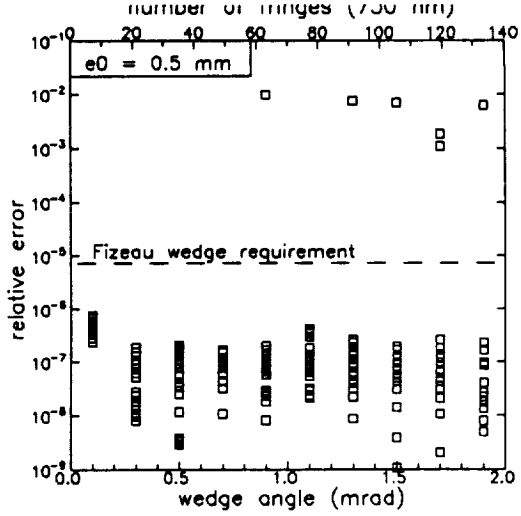

Figure 11. Optimization modeling results, measurement error versus Snyder wedge angle.

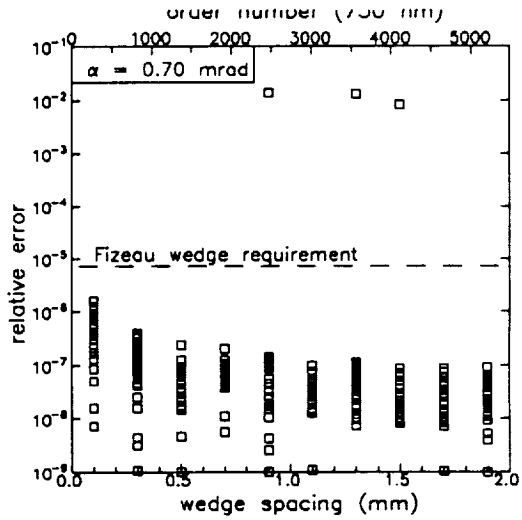

Figure 12. Optimization results, error versus Snyder wedge spacing.

A Fourier analysis of a real Snyder wedge interference pattern revealed that the noise background in the spectral region close to the fundamental frequency of the fringe pattern was far higher than was ever included in the modeling. Figure 13 shows the Fourier transform, obtained via a standard FFT, of a model fringe, a relatively severe case of artificially introduced noise and distortion. Figure 14 is the result of the same operation on a real fringe pattern, from an argon-ion laser source. (The analysis of a pulsed laser would yield a still higher noise background.) The principal observation here is the existence of a large background of noise with spatial frequencies close to the fringe frequency.

The source of this high spatial noise level is unknown. It is not even certain that this noise, as opposed to the broadening of the peak corresponding to the true fringe frequency, is responsible for the shortcomings of the Snyder wedge. A very useful exercise would be the repetition of the modeling work, using a noise background better matching the experimentally observed background. This could establish the role of the visually apparent background noise in disrupting the wavelength

measurement. The null results on optimizing wedge angle and spacing might also be affected by a realistic interference background, though some assumptions would be necessary concerning the effect of changes in angle and spacing on the frequency of the background.

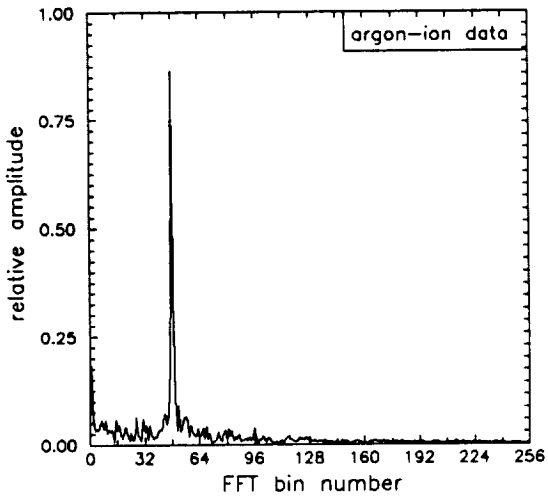

Figure 14. Fourier spectrum of a real Snyder-wedge interference pattern, cw laser.

Calibration and Testing of the Snyder Wedge

The Snyder wedge is calibrated using a long-cavity argon-ion laser. This laser lases on so many closely-spaced longitudinal modes simultaneously that the argon line width is filled, thus yielding lines with center frequencies determined by the atomic transition, rather than by cavity dimensions. The total line width is 4 to 6 GHz, or about 9 ppm of the central frequency or wavelength. This is comparable to the Snyder wedge accuracy anticipated, about 3 ppm.

Table I. Argon-ion wavelengths used in the Snyder wedge calibration.

Argon-ion laser wavelengths used in the Snyder wedge calibration. In column 1 the vacuum wavelengths of the principal lines are listed. In column 2 the wavelengths in air at 760 mmHg and 15 C, computed from the vacuum values, are listed. In column 3 the values for 760 mmHg and 20 C are listed. The values in column 4 are air-wavelength values from Reference 13. Columns 5 and 6 tabulate the differences, in parts per million, of the computed air wavelength values from the Chang values, an indication of the validity and reliability of the computed values.

vacuum	air(15)	air(20)	Chang	air15/Chang	air20/Chang
458.0630	457.9380	457.9401	457.9350	6.58	11.23
465.9198	465.7927	465.7948	465.7950	-5.02	-0.36
472.8186	472.6896	472.6918	472.6890	1.22	5.87
476.6194	476.4893	476.4916	476.4880	2.81	7.46
488.1225	487.9893	487.9916	487.9860	6.74	11.39
496.6462	496.5107	496.5130	496.5090	3.34	7.99
501.8558	501.7188	501.7212	501.7170	3.65	8.30
514.6742	514.5337	514.5361	514.5330	1.40	6.06

The vacuum wavelengths of the principal argon laser lines, and the wavelengths computed for air at 15 C and 760 mmHg, are listed in Table I. (The computer program for making this conversion, VAC_AIR.PAS, is included in the software delivered to NASA.)

The deviations of the lines from the air wavelength values tabulated in Reference 13 provided a valuable indication of the validity of the computed values. Reference 12, the Lasertechnics manual for their commercial Snyder-wedge interferometer, includes one spurious value. This presented some practical difficulties. The initial attempts to calibrate the Laserscope were frustratingly

unsuccessful, the determination of the wedge spacing yielding no valid solution. This problem was traced to the incorrect wavelength value, and correction of that value led immediately to good calibration results.

The calibration procedure developed for the Snyder wedge is a nearly automatic, two-step operation. First the normal Laserscope operation is pursued, using an argon-ion laser source, and storing the data obtained with the Laserscope, as the laser is tuned through the various lines. Then the program CAL_SNY is run, with this data file as input. The latter program has been set up to identify the various lines by a comparison of the Laserscope-indicated wavelengths with the values of Table I, with the assumption that the initial calibration is close enough to measure the wavelengths to within 2 nm. Since this is about 4000 ppm, a truly extraordinary event would be necessary to cause this assumption to fail. The CAL_SNY program executes the steps to be described in the paragraphs following, and, if the calibration is valid, updates the reference file, hdware.inf, which contains the Snyder-wedge calibration data.

The Snyder wedge calibration requires the determination of two parameters, the wedge angle and the wedge spacing (at some arbitrary reference point). In keeping with the two-pass functioning of the Snyder wedge, the calibration consists of two separate steps. The first yields the angle, the second the spacing.

The wedge angle appears in both the first-pass and second-pass wavelength calculations. The required accuracy of calibration of the wedge angle can be shown to be determined by the first pass. This first pass must, as Figure 1 indicates, deliver a wavelength accuracy on the order of 200-500 ppm. The wedge angle accuracy must be the same, since the wavelength is simply $2\alpha\Gamma$, where Γ is the fringe spacing. The error in wavelength due to error in α of the second pass is given by

$$d\lambda/\lambda = (\alpha x/e_s)\ (\delta\alpha/\alpha) \quad , \tag{8}$$

where x is the distance from the reference point. The second-pass wavelength must be accurate to ±2.5 to 7 ppm. The maximum value of x is one fringe spacing, since the maximum closest to the reference point is always selected for the second-pass calculation. This distance is, for the worst case (1000 nm wavelength and a full fringe spacing), 1 mm, and Eq. (8) indicates a specification $\delta\alpha/\alpha$ < 2500-7000 ppm, an order of magnitude greater than the tolerance required for the first-pass calculation. Thus an angle determination suitable for the first pass will be entirely adequate for the second pass as well.

The first-pass calculation involves only the angle, not the spacing. Thus the calibration procedure is neatly divided into a first-pass calibration, obtaining the angle to 200 ppm, and a second-pass calibration, obtaining the spacing to 2.5 ppm. The argon laser wavelengths, specified to about 0.2 ppm, should be adequate. The variation between 15°C and 20°C, about 5 ppm, is significant for the spacing only.

Snyder Wedge Angle Calibration

The essential output of the first-pass Snyder analysis is, as described above, the fringe spacing. The modeling, and other experimental results, show that the first-pass fringe analysis is capable of determining the fringe spacing and thus the wavelength to the 200-500 ppm required for successful functioning of this element. Presumably then the measurement of fringe spacing can, with known wavelengths, be used to determine the wedge angle, to the necessary accuracy.

The procedure for determination of the wedge angle is quite trivial. The Laserscope operating program stores data files including the node spacing, in pixels. A sample of the Laserscope data storage format is

1 13.3683897613 17.719391080 1236.648 764.105689 763.888002 15:16:41 14-7-1988
1 892 1.00

The first line consists of (1) the sequential shot number; (2) the location of the maximum used for the second-pass calculation, in pixels; (3) the node spacing, in pixels; (4) the order number of the maximum used for the second-pass calculation; (5) the first-pass wavelength, in nm; (6) the second-pass wavelength, in nm; and (7) the time and date. The second line is Fizeau wedge information, which for the moment is irrelevant.

The Snyder-wedge calibration program, CAL_SNY, first reads a reference file, LAMBDA.LST, of the known argon-ion laser wavelengths. Then it reads the data file created by the Laserscope operating program, consisting of pre-calibration measurements of the argon-ion wavelengths. From the latter it extracts the fringe spacing (twice the node spacing), and the computed second-pass wavelengths.

By comparing the computed wavelength to the argon-ion air-wavelength values, CAL_SNY determines the exact wavelength corresponding to each measurement. (This is the key to making a calibration routine which does not require the operator to provide the specific wavelengths of the measurements.) Then the apparent wedge angle for each measurement can be computed, from $\alpha = \lambda/2\Gamma$. These apparent values are simply averaged to obtain the net value of α. As elementary as this procedure is, there is no better way. The simple average is also the least-squares fit of a constant to a set of data.

Figure 15 illustrates this first step of the calibration. The apparent wedge angle, $\lambda/2\Gamma$, is shown for the sequence of argon-ion laser wavelengths. The solid lines indicate the range of error allowable for the wedge angle. Each wavelength consists, in this example, of five successive measurements of the laser wavelength. Clearly the scatter within each wavelength set is very small, much smaller than the variation from wavelength to wavelength. This is an encouraging indication of the short-term stability of the apparatus, and the minimal effect of random noise in the system.

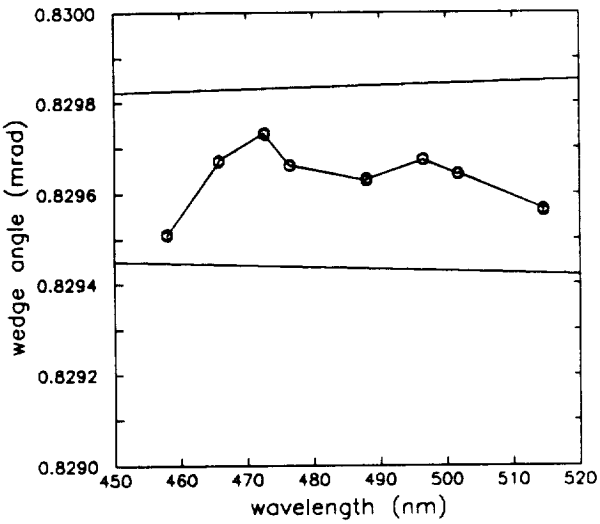

Figure 15. Snyder wedge angle calibration, argon-ion laser spectrum.

The variation with wavelength is more troublesome. The first tests of this sort showed a consistent dependence of angle on wavelength, apparently a linear variation of effective angle with wavelength. This was very disturbing, since an extrapolation of the angle beyond the rather limited range of argon-ion wavelengths rapidly exceeded the allowable bounds. After the possibility of dispersion in the fused silica of the interferometer was eliminated, the problem was tracked to an optical alignment adjustment.

Experience shortly revealed that this apparently simple calibration step was in fact a crucial part of the procedure, presenting problems that were never satisfactorily resolved. Figure 16 shows the same data, now on the full wavelength scale of the instrument. Clearly the argon-ion data cover only a very small range of wavelengths, and the variations are great enough that extrapolation of a calibration from the 500 nm range to the near infrared is very unreliable.

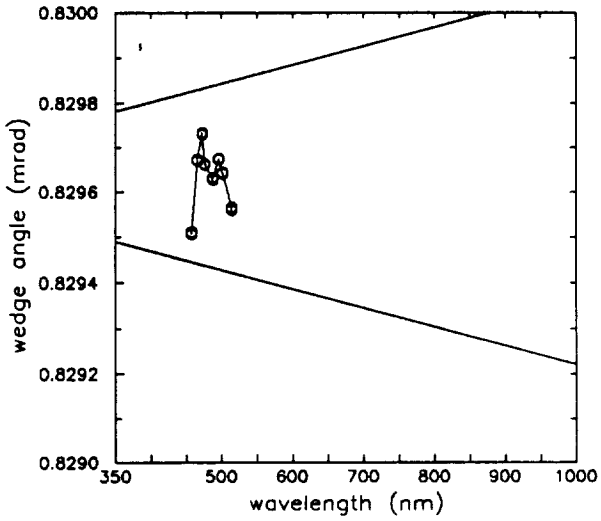

Figure 16. Snyder wedge angle calibration, full spectrum.

The shortest wavelength of the argon-ion laser, 458 nm, always yielded an apparent wedge angle lower than that of the other wavelengths. If this one point is arbitrarily removed, the others show a clear linear trend with a slope far from zero. One possibility, never eliminated, is that the 458 nm data are spurious, and the remaining points, indicating a wavelength-dependent wedge angle, suggest a misalignment. The later measurements with a dye laser, in the near infrared, support this interpretation. This issue might be resolved only by the extension of the Snyder-wedge calibration procedure into the infrared with some well-established laser lines.

Under the circumstances, and with no good reason for removing the 458 nm argon line, the instrument was aligned for the best apparent calibration over this limited spectral range. The problem of an apparently wavelength-dependent wedge angle is so critical that a display of this information was incorporated in CAL_SNY, as illustrated in Figure 17. This is a video dump of the display upon completion of the calibration. The upper-left window is the display of apparent wedge angle, drawn against the simple sequence of input data sets (not wavelength). All these points must lie within the allowed range of variation, arbitrarily set to ±280 ppm, or the calibration will be rejected. The operator can decide whether the calibration is good, and permit the program to update the hardware information file. The display shown in Figure 17 is the same data as shown in Figure 15 and Figure 16. While this appears from the display to be a

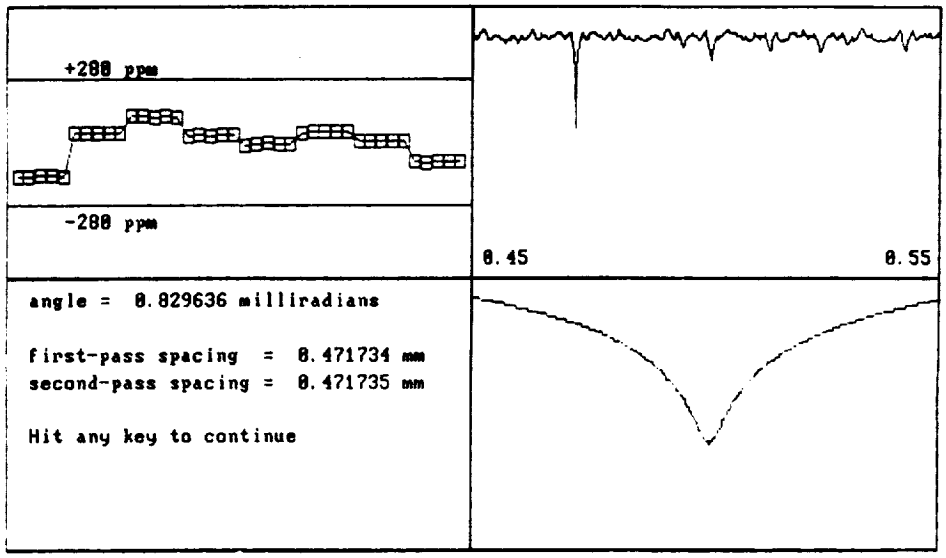

Figure 17. Video display, Snyder wedge calibration.

very good calibration -- this is in fact one of the better calibration runs -- it must be kept in mind that the extrapolation to long wavelengths remains suspect.

Snyder wedge spacing calibration

The wedge angle is set entirely by the first-pass, fringe spacing measurement, since the angle appears in such a weak manner in the second-pass wavelength evaluation.

The wedge spacing is found by the laborious but straightforward "method of exact fractions" [14]. A spacing is assumed, taking for convenience a value obtained by assuming an integral order number for one wavelength of the set. Then the order number, integer plus fraction, is determined for the other members of the calibration set, using the known wavelengths. The fractional parts are ideally zero, if the spacing is correct. If the order number assumed for the first wavelength is incorrect, and the spacing thus also incorrect, then the fractional parts of the order numbers for the other wavelengths will be nonzero. A sum of squares of the fractional parts of the order numbers for the other members of the set is an indication of the deviation of the spacing from the correct value.

The upper-right window of the calibration display, Figure 17, is this sum of squares of fractional parts, on a logarithmic scale. The spacing is stepped from 0.45 to 0.55 mm, in intervals of a change in order number of unity at the first wavelength in the calibration set. A sharp minimum is clear in the display of Figure 17. This is a certain indication of a good solution to this problem. (The spurious wavelength value for one of the argon-ion lines given in the Lasertechnics manual was exposed by the failure of this technique to yield a good solution, a failure immediately solved when the wavelength value was corrected.)

This first exercise of the least-fractions method steps the wedge spacing by half the wavelength of the first calibration data, or about 200-250 nm. As a refinement of this procedure, the spacing is stepped around the best value found by this process, but now with a step size of 0.2 nm. This expansion of the minimum of the upper-right window is displayed in the lower-right window. Ordinarily the change in the spacing value obtained by this "microstepping" procedure is quite small. As this example shows, the change as a result of this refinement is only 1 nm, or 2 ppm. (In fact, the change was 0.06 nm, or 1.3 ppm. The next decimal place is preserved internally, but not displayed.)

If a calibration is attempted with an insufficient number of wavelengths, the least-fractions display will show more than one minimum. The solutions to this algorithm are periodic. If only two wavelengths are employed, the display of Figure 17 will show a regular sequence of cusps, with the period being a function of the difference between the wavelengths. It is essential to have a number of wavelengths, with differing solution periodicities, so that the multiple solutions are reduced to a single solution. Six wavelengths appears to be a satisfactory number. Fewer can be used if one has additional information in order to select the correct minimum from a number of similar minima. The calibration program, CAL_SNY.COM, produces an output file, CAL_SNY.DAT, which contains the wedge-angle results for all of the data sets, and the first-pass and second-pass wedge spacing values. First-pass and second-pass refer, in this context, to the "coarse" and "fine" applications of the least-fractions technique.

Snyder Wedge Performance with a Pulsed Laser

The objective of the instrument is, of course, wavelength measurement of a pulsed laser source. The test and evaluation of the Laserscope was done using a YAG-pumped dye laser. The wavelength of the dye laser was determined by observation of the absorption of a small sample of the output by a long air column. Water vapor absorption in the air column indicated the tuning of the laser through well-known molecular absorption lines.

This arrangement was not perfectly satisfactory since the dye laser, like most dye lasers, produced an output with multiple transverse modes, rather than the ideal TEM_{00}. The strong pinhole filtering of the Laserscope, required to obtain high collimation of the input, discriminates against transverse modes. Thus the spectrum being sampled by the Laserscope was not identical to the spectrum of the unfiltered light. The wavelength spacing of the transverse modes was small, perhaps hundredths of a wavenumber, or on the order of 1 ppm of the fundamental wavelength. Thus the Snyder wedge should be little affected by this difference. The first pass Snyder calculation in particular is much too insensitive, at 200-500 ppm accuracy, to be disturbed by such a small wavelength variation.

The dye laser was operated around a series of water-vapor lines at 764 nm wavelength. This is well separated from the calibration range of 450-540 nm. As is clear from Figure 16, an extrapolation of the argon-ion calibration to the near infrared depends on whether the 458 nm point is valid. If it is not, then the remaining points show a strong slope, more than sufficient that the first-pass results would be in error at 764 nm by an amount exceeding the allowed range. This would be due to a misalignment due to the invalid point. A calibration operation including lines in the IR as well as the blue would avoid this problem.

Figure 18 shows the results of the first-pass Snyder wedge wavelength measurement on this dye laser system. At this wavelength the accuracy of this first pass must be within ±410 ppm in order to get the correct order number in the Snyder wedge. It is clear that the error in the first-pass measurements is excessive, and the wavelength calculations which follow this first step will be erroneous.

Two observations, of central importance for the possible extension of this instrument to an improved version, are to be gleaned from this figure.

First, the consistent deviation from zero discrepancy is clearly a calibration problem. As described immediately above, the calibration is performed in the blue-green end of the spectrum, at 460-510 nm, while these measurements are performed in the near infrared, at 764 nm. It is the extrapolation of the calibration over this limited spectral range that causes the systematic divergence of the measurements from the correct values, and a better calibration source, one with calibration lines close to both ends of the spectrum, would presumably eliminate this problem.

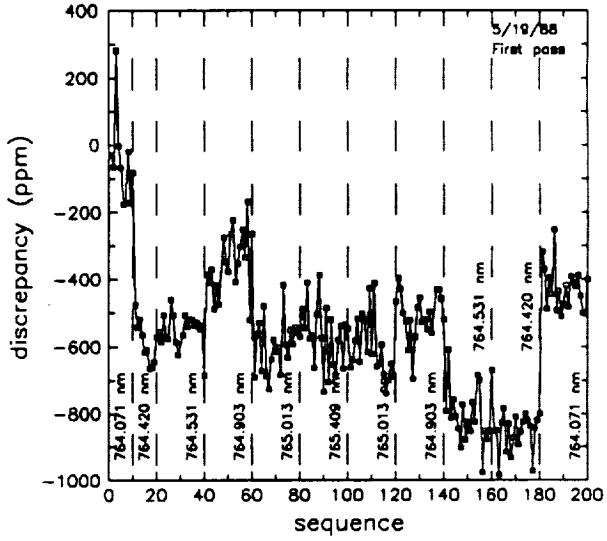

Figure 18. Snyder-wedge first-pass results, pulsed dye laser.

The leftmost points of Figure 18, at 764.071 nm, require specific explanation. In setting up the instrument for these measurements it became evident, from the real-time display, that the order number obtained from the first-pass Snyder measurement was in error by unity. It was found that an exceedingly fine adjustment of the optics -- in fact a tightening of a screw, not a recalibration adjustment -- was sufficient to bring about a correct order number. Thus the first data points taken (the scan is simply chronological from left to right) are close to the correct values.

Upon closing up the Laserscope for taking the full series of measurements, this tightening of an optical mount screw relaxed, causing the optics to revert to, presumably, the original positions. This is the meaning of the sharp change in the discrepancy data between the first set of points, at 764.071 nm, and the second, at 764.420 nm. This is further indication that the problem in the first-pass Snyder wavelength evaluation is a calibration issue, and not an inherent inaccuracy of the apparatus. This also suggests the extremely exacting alignment demanded by the Snyder optics.

Second, the scatter, or nonsystematic variation of the data, is within the ±410 ppm range -- but just barely. The scatter within each wavelength set is less than ±100 ppm, but there are significant changes in the central value at each wavelength, a variation of unknown origin, such that the total range of variation of the data is about 800 ppm. Evidently this system would be subject to occasional order-number misses even if the calibration problem were solved.

From these observations we draw to conclusions, pertinent to any redesign of this instrument.

(1) A calibration method must be devised which provides calibration wavelengths near both ends of the operating spectrum. The leverage in attempting to extrapolate from a few data near one end of the spectrum, to the other end, is simply too great.

(2) The variation in first-pass measurements, with the offset due to the calibration problem removed, is close to the maximum tolerable. The most direct approach to resolution of this problem is the use of a Snyder wedge with still smaller spacing, i.e. 0.25 mm instead of the current 0.5 mm (nominal).

In view of these results it should not be surprising that commercial wavemeters based on this technology, using 1 mm Snyder wedges, have been less than fully successful. Unofficial discussions with a former engineer of a company currently producing a Snyder-wedge wavemeter confirm that, were they doing this design again, they would reduce the design specifications of the instrument.

Because of the calibration-induced offset, the first pass of the Snyder measurement yielded order numbers erroneous by unity in most of the measurements. As a means of evaluating the second-pass performance independently of the first-pass difficulties, the incorrect order numbers were manually corrected, and the deviations of the second-pass measurements computed as if the first pass had performed adequately. The results are shown in Figure 19.

The accuracy required of the second pass is determined by the spacing of the Fizeau wedge. This is ±5.5 ppm for the 3.5 cm wedge used in the prototype Laserscope.

It is evident that there is a consistent offset, of some 30-35 ppm, well beyond the amount allowed. While it is tempting to attribute this to a calibration limitation, as is certainly the case for the first pass, it is not so clear that the limited spectral range of the calibration should be important. The calibration of the wedge spacing, for the second-pass calibration, is virtually independent of the calibration of the wedge angle, the first-pass calibration. If the order number has been correctly obtained, via the least-fractions procedure, then the spacing should be correct, as accurate as the

calibration wavelengths. As was shown in connection with Eq. (8), the uncertainty in the wedge angle α, now due to the calibration problems of the first pass, has little effect on the second-pass evaluation, and consequently little effect on the wedge spacing.

On the other hand, the tightening of the optics mount screw to repair, temporarily, the order-number missing of the first-pass wavelength calculation, had a similar effect on this second-pass evaluation, even though the wedge spacing cannot possibly have been affected by this mechanical change. It appears to us that there is another alignment factor here, and that the discrepancy induced by a very fine alignment error is wavelength dependent, similar to that observed in the first pass.

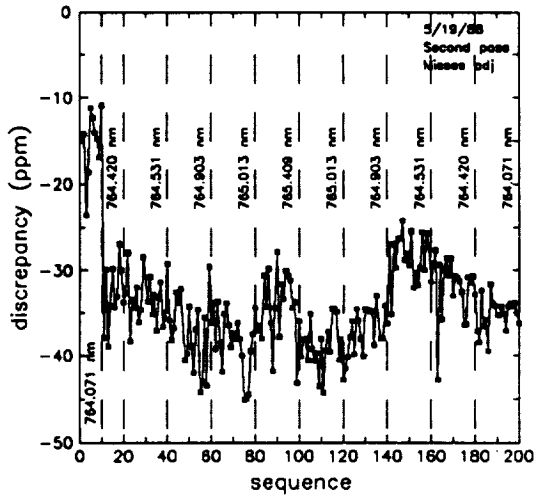

Figure 19. Snyder second-pass results, pulsed laser.

Thus the best interpretation of the results shown in Figure 19 is that there again is a problem associated with the limited spectral range of calibration. A calibration over a wider spectral range would reveal misalignments which yield apparently wavelength-dependent wedge angle and spacing.

The nonsystematic variation in the second-pass results, with the consistent offset removed, amount to roughly ±10 ppm. This is about twice the tolerable amount for the 3.5 cm Fizeau wedge. The high-resolution optical interferometer would have to be reduced to 1.8 cm or less in order for the Snyder to obtain, reliably, the correct order number.

The evaluation of the first-pass uncertainty indicated that the Snyder wedge spacing should be reduced, perhaps by half. The effect on the random variations evident in Figure 19 of this change is not entirely predictable. If these variations are due to an effective change in wedge spacing, the wavelength error is given by

$$\delta\lambda/\lambda = \delta e_s/e_s \quad . \tag{9}$$

If the apparent changes in wedge spacing are proportional to the spacing, then the proportionate variation in measured wavelength is unchanged.

On the other hand, if the variations are due to fringe location errors, and are unchanged by wedge spacing, then the effect on wavelength accuracy is inversely proportional to the wedge spacing:

$$\delta\lambda/\lambda = \alpha\delta x/e_s \quad , \tag{10}$$

and decreasing the Snyder wedge spacing will increase the relative wavelength error in the same proportion.

Thus a Snyder wedge with half the spacing might have either the same proportionate wavelength error, ±10 ppm, or twice that, ±20 ppm. In the former case, the Fizeau wedge would have to be 1.8 cm or shorter; in the latter, 0.9 cm or shorter. Thus the resolution of the Fizeau element might

be somewhat reduced, though, as will be described in the following sections, not as much as the spacing ratios suggest.

Snyder Wedge Summary

Clearly the Snyder wedge does not perform nearly as well as anticipated. This element was supposed to provide wavelength measurement with about ±5 ppm accuracy, sufficient for order number determination in the Fizeau wedge. This appeared to be a very reasonable goal, since other builders of Snyder-wedge interferometers have claimed accuracies of 1 ppm [8] and 2 ppm [9]. In fact, due to calibration difficulties, the element is reliable only within a narrow spectral range, and the accuracy with a pulsed laser appears to be no better than ±10 ppm.

The recommended steps for the development of a more reliable pulsed-laser instrument are:

(1) development of a calibration technique employing lines ranging across the spectrum of the instrument, from the blue to the near infrared;

(2) reduction of the Snyder wedge spacing from 0.5 mm to 0.25 mm, possibly compromising the ultimate accuracy of the stage but increasing its reliability and decreasing, presumably, the alignment delicacy; and

(3) reduction of the spacing of the high-resolution, Fizeau interferometer to match the capabilities of the Snyder wedge, i.e. from the current design value of 3.5 cm to perhaps 1 cm.

It seems assured that these steps would yield a Snyder-wedge wavemeter with reliable pulsed-laser accuracy of ±10 to ±20 ppm.

There remains the question of why other builders appear to have had better results, with 1-2 ppm accuracy claimed. The off-axis parabolic mirror used in our design was not satisfactory, defects in the surface producing structure in the interference patterns, i.e. speckle due to interfering scatter. The advantage of the mirror is that it obviates the dispersion of a collimating lens. In retrospect, dispersion would have been easier to deal with, incorporating software calibration factors, than were the alignment and scatter-site defect troubles of the paraboloid. One other builder of Snyder wedge interferometers attempted, then rejected, the off-axis parabola, due to "striations which produced unacceptable artifacts in the collimated beam" [5]. Thus the shortfall in accuracy of our Snyder wedge might be wholly due to the mirror, and the substitution of a lens could yield an instrument more accurate and easier to align.

Fizeau Wedge: Theory of Operation

The (multibeam) Fizeau wedge consists of high-reflectance flats tilted by a small angle α. This device has been analyzed by many workers [15] and currently finds its principal application in the testing of optics. The Fizeau wedge was selected here over the more conventional Fabry-Perot interferometer due to the good match with linear, self-scanning photodiode arrays and the compact optical structure. The principal issue is the compromise in potential finesse, the sideways translation of successive reflections limiting the number of reflections contributing effectively to fringe formation [16]. An essential question is the value of this finesse, and corresponding spectral resolution, limit. A technique has been devised for the convenient optimization of all the variable parameters of the Fizeau wedge -- the spacing, wedge angle, face reflectance, and tilt -- for achieving the maximum possible wedge resolution.

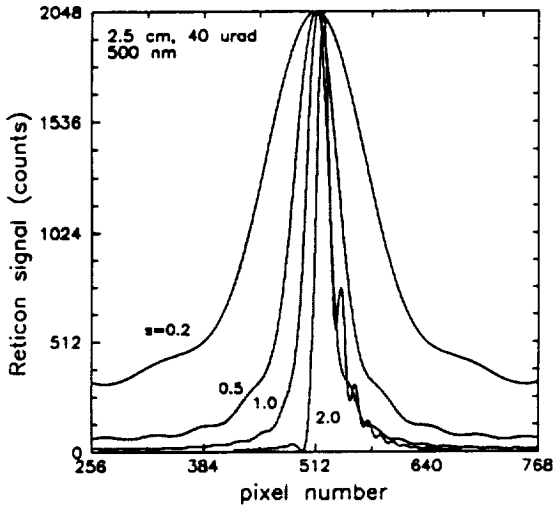

Figure 20. Fizeau wedge fringes versus shape factor.

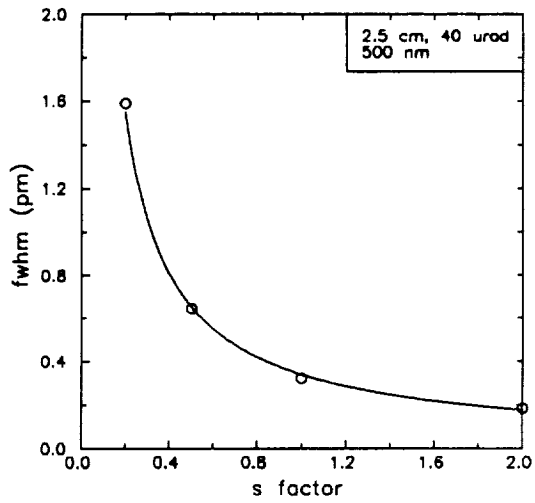

Figure 21. Fizeau fringe full-width half-maximum, versus shape factor.

Fizeau-wedge fringes can be described by a single "shape factor" s, given by

$$s = (m_0\alpha^2)^{1/3}F_A \qquad (11)$$

where m_0 is the order number of the interference fringe ($m_0 = \lambda/2e_0$, λ being the wavelength and e_0 the wedge spacing) and F_A is the Airy finesse ($F_A = \pi R^{1/2}/(1-R)$, where R is the wedge face reflectance, assumed identical for the two faces). A large value of s corresponds to high interference and relatively large transverse displacement of successive reflections. Figure 20 shows Fizeau fringes computed for various values of s, varying the face reflectance alone. These fringe computations employed a prescription by Meyer [17], corrected for an error in the phase evaluation of the reflected waves. A small value of s, 0.2, corresponds to a smooth, broad fringe, somewhat asymmetric but not very different from the Airy form. As s, and the number of interfering reflections, increases, the fringe becomes narrower, and develops additional structure, secondary maxima, on the wider direction of the wedge. Beyond s=2.0, the higher-order reflections contribute only to reinforcement of this secondary structure, and do not further narrow the principal maximum. This outcome is more clearly shown in Figure 21, where the full-width half-maximum of the fringes is plotted against s. Clearly the resolving power of the Fizeau wedge is not significantly enhanced by an increase of s above 2. This in turn corresponds, via Eq. (11), to a maximum useful face reflectance for a given wedge spacing and angle.

It is well known that tilting the Fizeau wedge will sharpen the fringes. The wedge angle causes successive reflections to be deflected towards the wide end of the wedge, each reflection angle increasing by 2α. If the wedge is tilted by an angle θ such that the initial translation of successive reflections is towards the narrow end of the wedge, then after $\theta/2\alpha$ reflections the sideways translation of successive reflections will be reversed, thus compensating in part for the imperfect superposition of reflections. Langenbeck [18] proposed that the ideal tilt angle should be $2^{1/3}\alpha F_A/s$. Our computations have shown that this tilt is very close to the point of fringe collapse, and a tilt angle of 0.80 the Langenbeck value provides good fringe stability with negligible decrease in resolution. This tilt has been used in calculating the fringes of Figure 20.

Based on the Meyer modeling results a simple map of Fizeau-interferometer operating parameters can be drawn, Figure 22. The abscissa is the Airy finesse F_A, a measure of the face reflectance, while the ordinate is the order number $m_0=2e_0/\lambda$, a measure of the wedge spacing. The effective resolution $\delta\lambda/\lambda$ is obtained from the Meyer model, and fixed values of $\delta\lambda/\lambda$ yield the lines labeled with the resolution in parts per million. The relationship between m_0 and F_A is fixed by the shape factor. Lines for various values of wedge angle are shown. Finally, the wedge spacing, for a specified wavelength λ, determines the order number m_0. Figure 22 shows m_0 for a spacing of 25 mm and wavelengths 350, 750, and 950 nm.

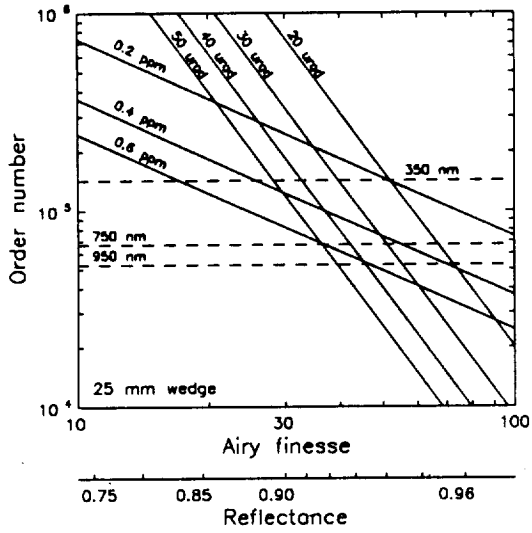

Figure 22. Map of Fizeau interferometer parameters, 25 mm wedge.

The operating point for a given wedge is the intersection of the line for a fixed wedge angle and the line for a fixed wedge spacing. For example, if the wavelength is 750 nm and the spacing 25 mm, $m_0=6.667\text{x}10^4$, a line which intersects the 50 μradian line at about $F_A=36$. This indicates that the reflectance of the wedge must be 0.92 to obtain the specified shape factor, 2.0.

The resolution will be given by the value of the effective resolution line which passes through this point. If a certain resolving power must be achieved or exceeded, then this operating point must lie above the corresponding resolution line. The operating point determined in the paragraph above is close to the 0.6 ppm line, indicating that the full-width half-maximum of the fringe will be 0.45 pm.

If higher resolution is needed, the operating point must move to a higher resolution line. This may be achieved by moving to the right, i.e. higher face reflectance, or by moving up, i.e. greater wedge spacing. Movement of the operating point in either direction entails a decrease in wedge angle to maintain constant shape factor. However, the wedge angle cannot be decreased without limit, since detector lengths are limited and one must have at least one full fringe on the detector for every wavelength under consideration. One must have $\alpha>\lambda/2W$, where W is the length of the detector, and λ is the longest wavelength to be observed. This typically evaluates to tens of microradians. For a maximum wavelength of 1000 nm, and a detector of 1024 elements, the minimum wedge angle is 20 μrad (25 μm pixels) or 38 μrad (13 μm pixels).

From Figure 22 it can then be deduced that the best possible resolution, at 750 nm, will be about 0.33 ppm (20 μradian angle) or 0.50 ppm (38 μradian angle). These fringe width values correspond to effective interferometer finesses of 46 and 30, respectively. The smaller wedge angle leads to a higher potential finesse because it permits a higher face reflectance, and thus Airy finesse. The limiting Airy finesse increases as the wedge angle to the -2/3 power.

Increasing wedge spacing is an obvious means of increasing absolute resolution, at the expense of free spectral range. Figure 23 shows the Fizeau operating map with lines for a 35-mm wedge superimposed. The maximum wedge angles are unchanged by the increase in spacing. The 750 nm resolution for a 20 μradian wedge will be about 0.26 ppm, and for a 38 μradian, 0.40 ppm, for effective finesses of 41 and 26, respectively.

These results are summarized in Table II. The design objective was a resolution of 0.3 pm, or 0.40 ppm at 750 nm. Evidently the 25 mm wedge with the larger detector array, or the 35 mm wedge with the smaller, would ideally be capable of the specified resolution.

The choice was made on the basis of the wedge diameter issue. The smaller detector permits a smaller wedge diameter, with less potential difficulty with wedge flatness. The smaller detector diameter also reduces the problems of beam expansion, many laser beams being considerably less than 2.5 cm in diameter. The increased wedge length presented little difficulty. Thus the 35 mm wedge and 1024x13 μm detector were chosen. The face reflectance required for a shape factor of 2.0 was 0.920.

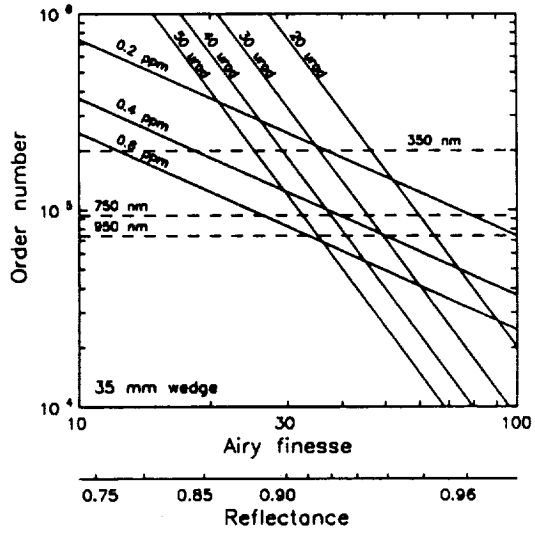

Figure 23. Map of Fizeau operating parameters, 35 mm wedge.

Fizeau Analysis Algorithm

The analysis of the Fizeau patterns is straightforward, far simpler in concept than the Snyder analysis. The principal difficulty is the identification of true peaks versus spurious maxima. It was necessary to devise criteria by which the software could judge whether a local maximum was a legitimate Fizeau interference peak, or merely noise. Having identified a peak, the problem was deconvolution of multiple fringes due to multiple laser modes. A further issue was the distinction of multiple orders of the Fizeau wedge. These problems led to building "judgment" into the program, somewhat arbitrarily.

Table II. Fizeau modeling results.

Fizeau modeling results, for wedges of 25 and 35 mm spacing, and angles of 20 and 38 μradians. The smaller angle corresponds to the maximum permitted with a 1024x25 μm detector array, the larger to the maximum angle permitted with a 1024x13 μm detector array. Tabulated here are the anticipated resolution, in parts per million at 750 nm, and the effective finesse, defined as the free spectral range divided by the fringe full-width half-maximum.

	α=20 μrad		α=38 μrad	
	fwhm/τ	finesse	fwhm/τ	finesse
25 mm:	0.33	46	0.50	30
35 mm:	0.26	41	0.40	26

The procedure (embodied in the subroutine FIZEAU.PSL) is as follows.

(1) The raw fringe data are smoothed by simply taking the average of each pixel with the two adjacent pixels. This eliminates odd-even pixel noise, which was a problem before this step was added.

(2) The maximum along the array is located. The array ends are excluded from this search in order to avoid an attempted deconvolution of a partial fringe, right at the detector end.

(3) A window is defined around the maximum, plus and minus 300 pixels. This is to avoid confusing distinct orders of the Fizeau wedge.

(4) The baseline is subtracted off to refer the fringe to zero.

(5) A minimum legitimate peak height is defined as one-fourth of the maximum fringe height. If this is less than 256 counts, the minimum is set to 256. This is to avoid the software being trapped by small noise pulses.

(6) Starting from the left edge of the window, the first maximum above this minimum legitimate height is located. This is done by the procedure PEAK_FND.PSL. The height and location of this peak will be retained for fringe amplitude and wavelength determination.

(7) A reference pattern stored in the machine (in the file fizeau.ref) is scaled and shifted to match the peak identified in (6). This is done with integer arithmetic, with a resolution of about 6 bits (1/64). The scaled and shifted reference pattern is subtracted from the window region to leave a residual fringe pattern.

(8) Steps 6 and 7 are iterated to locate additional fringes. This may be repeated for a maximum of three fringes, after which the software arbitrarily terminates the deconvolution.

It is essential that the fringe pattern stored in fizeau.ref be a valid representation of the ideal fringe produced by the Fizeau wedge with a narrow-line input. If the stored fringe is narrower than the experimental fringe, then subtraction will leave a large residue in the original location. This residue will generate spurious peak identifications. On the display, this will be evident as multiple lines on a single, broad fringe.

The stored fringe must also have the correct secondary maximum structure of the Fizeau fringe. When operating correctly, this procedure will subtract off the secondary structure from an experimental fringe and leave zero, avoiding the mis-identification of the secondary maxima as additional, low-amplitude fringes.

Calibration and Testing of the Fizeau Wedge

Figure 24 shows an interference pattern from the Fizeau wedge with a tunable helium-neon laser source, wavelength 593.937 nm. The two longitudinal modes of the laser are clearly evident. Also evident are the secondary maxima characteristic of the multibeam Fizeau wedge.

The fringes computed with the theoretical model, for wedge spacing and angle as later deduced (35.95 μradians angle and 35.066 mm spacing), for the nominal reflectance of 0.92, and for a tilt of 0.80 of the Langenbeck value, are also shown. The two modes were assumed to be separated by 438 MHz, according to the specifications of the laser manufacturer.

The agreement in fringe shape is quite satisfactory. The tilt of the wedge in the experiment was probably a little less than the value assumed in the calculation, reducing the amplitude of the secondary structure.

Two orders of the Fizeau wedge should appear here. The first fringe, or pair of fringes, is not as strong in the experimental data as it should be. The calculation is incomplete in this region due to the manner of constructing the fringe for the second mode, and a full fringe should appear at the left end of the wedge. That it does not was invariably observed, and indicates some aperturing of the beam incident on the Fizeau wedge.

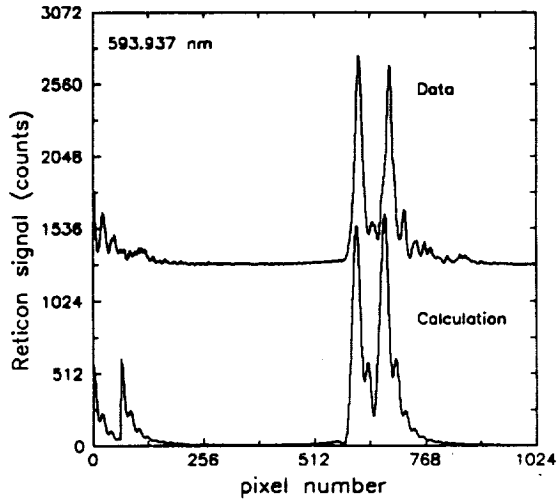

Figure 24. Fizeau interference patterns, experimental and calculated.

The experimental fringe width is 21 pixels. This is equivalent to 0.169 pm, or 0.29 ppm of the wavelength, or 0.0048 cm^{-1}. The objective was 0.30 pm, and is evidently achieved with this interferometer. The effective finesse of this device, defined as the free spectral range divided by the fringe full-width half-maximum, is 30. An essential property of multibeam Fizeau wedges, borne out by these experimental results, is that the limiting finesse is quite modest, considerably less than is achievable with Fabry-Perot interferometers. The advantages of the Fizeau are linear dispersion and compactness, not resolution capability.

The Fizeau wedge angle was deduced not from the helium-neon data but from the Fizeau mode spacing with pulsed-laser input. There are three reasons for selecting this technique over calibration with the longitudinal modes of the HeNe laser. First, the spacing of Fizeau modes is independent of the wedge thickness, while the spacing of laser modes with a common Fizeau mode number is not. Second, the spacing is much greater, almost the full length of the detector, permitting a more accurate resolution of the spacing. Third, the reliability of the longitudinal mode spacing frequency specified by the helium-neon laser manufacturer is unknown, while the dye-laser wavelengths, locked to water-vapor absorption lines, are very well known. Against these considerations must be weighed the distortion of the second Fizeau mode. Figure 25 shows a relatively good case of two Fizeau orders with the dye laser.

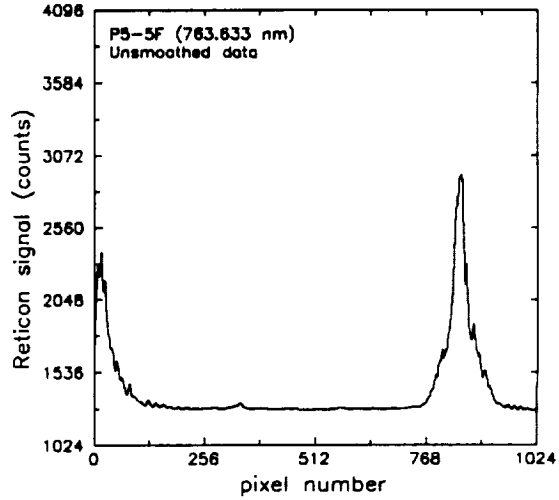

Figure 25. Fizeau fringes, pulsed dye laser.

The wedge angle obtained from the pulsed laser measurements was 35.95 μradians, ±0.5 μradian. This is an uncertainty of about ±1%, an acceptable value since the wedge angle figures only very weakly in the wavelength measurement. The ratio of uncertainty in wavelength to the uncertainty in wedge angle α is $\alpha x/e_p$, where x is the distance from the reference point. For a maximum value of x, this coefficient is 1.3×10^{-5}, so the uncertainty in wedge angle contributes a maximum uncertainty in wavelength of less than 0.2 ppm. The accuracy goal was 0.2 ppm, so this is not negligible, but is a worst-case value.

The fringes of Figure 25, a reasonably typical example of pulsed-laser Fizeau fringes, display a great degradation of fringe quality. The cw-laser fringes of Figure 24 are quite close to the ideal shape, including fringe narrowness and the secondary structure. The pulsed dye laser system, described in the section on the performance of the Snyder wedge with pulsed sources, invariably yielded broad fringes.

The calibration of the wedge angle was done by hand, using sets of data such as shown in Figure 25. This procedure required so much judgement that automation in a computer program was not feasible. Some software tools are necessary for this operation, and will be described here.

Two forms of data files are produced by the Laserscope operating program. The Limited storage option yields short data files consisting of only the information header and the reduced wavelength data, i.e. the Snyder wavelength, and the number and location of Fizeau fringes, after deconvolution. The Full storage option saves long data files including the same information plus the raw fringe data, both Snyder and Fizeau. The Limited storage is used when one wishes to save only the essential laser performance data, as when monitoring a large number of shots for laser stability or analysis work. The Full storage is necessary when a detailed analysis of the fringes will be required, as when doing a calibration of the Fizeau or Snyder wedges.

Because the files saved by Laserscope include both text and numeric information, the files are text files, which can be read by any utility editor, including EDLIN. Ordinarily the files will consist of a number of laser pulses stored in sequence. One simple procedure for extracting the data from a single pulse is to use the editor to copy the selected lines into another file. This is very tedious for more than a couple of pulses, and, if done with an editor restricted to line moves like EDLIN, does not yield a file ready for display. (Many editors exist which are far easier to use and much more powerful than the very primitive EDLIN. Kedit and Brief are just two very good alternatives.)

FILESPLT is a program written to automate the extraction of single data files from the concatenated files produced by Laserscope. This will take the information header at the start of the file, and the two-line run summaries at the start of each data set, and save them in a file with the extension .HDR. (The file name is chosen by the user.) The Snyder data and Fizeau data for each run are separated and saved in a sequence of data files, e.g. P5-5Snn.DAT, P5-5Fnn.DAT, where "nn" is a counter of the data files, beginning with one.

These separated data files may be displayed directly with the program VIEW. A video dump is incorporated into the graphics system, and pressing Shift-PrtSc will yield a printer record of the display.

Occasionally it is necessary to go through the data of a run manually, locating features precisely. The determination of peak locations from data such as shown in Figure 25 is an example. However, the data files produced by FILESPLT cannot be read by an editor because these files are, for conservation of disk space, binary, not ASCII. Another program, FILECONV, was written to convert files from binary to ASCII (and vice versa).

This may be sufficient, since one now has a data file consisting of the integers produced originally by the digitization of the fringes. It is convenient, and for some purposes necessary, to add a column of the pixel index. INTADD adds this column, a simple sequence of integers counting from 0 to 1023, to the integers of the fringe data. Thus one finally has an editor-readable data file consisting of both x and y values for the fringe data, Snyder or Fizeau, depending on the file selected after FILESPLT.

Yet another utility program, now primarily of historical interest, is SMOOTH, which reads a file of y-value integers only (i.e., the data file produced by FILECONV) and performs the same smoothing operation employed in the Laserscope Fizeau analysis. This smoothing was introduced to eliminate odd-even pixel noise, and amounts merely to averaging a pixel with its two neighbors. Odd-even noise is thus perfectly eliminated with minimal effect on the fringe information. The arithmetic performed is y_av := y0 + y2 + (y1 shl 1), where y1 is the pixel of interest, and y0 and y2 are the preceding and following pixels. The y1 shl 1 operation is a very fast multiplication by two, and this average is in fact (y0+y1) + (y1+y2). This sum is clearly four times the true average of the three pixels; the division by four was left out, since this rescaling of the data has no effect on the peak location or relative amplitude determinations.

SMOOTH also inserts the pixel-count integer. In general, Fizeau fringes will benefit from the smoothing operation, and the use of SMOOTH instead of INTADD will produce data files more easily analyzed.

Figure 26 shows the data of Figure 25 after smoothing. The two Fizeau mode peaks are found at pixels 17 and 848. The wedge angle thus evaluates to 35.43 μradians. The full-width half-maximum of the principal fringe is 35 pixels, equivalent to 0.28 pm. Compare the fwhm of the fringe with the cw source, 21 pixels, or 0.17 pm. This broadening of the fringe with the pulsed laser source was always evident.

The source of this broadening is presumably the laser itself, which runs on numerous closely-spaced transverse modes. Figure 27 shows a superposition of ten successive pulses from the dye laser, under identical conditions and very

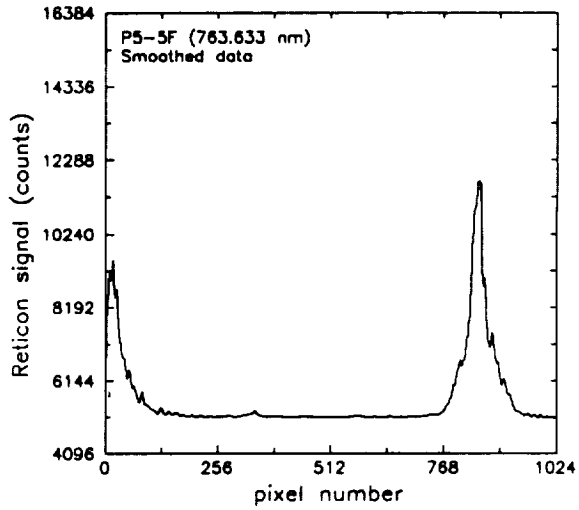

Figure 26. Smoothed Fizeau fringes (angle calibration).

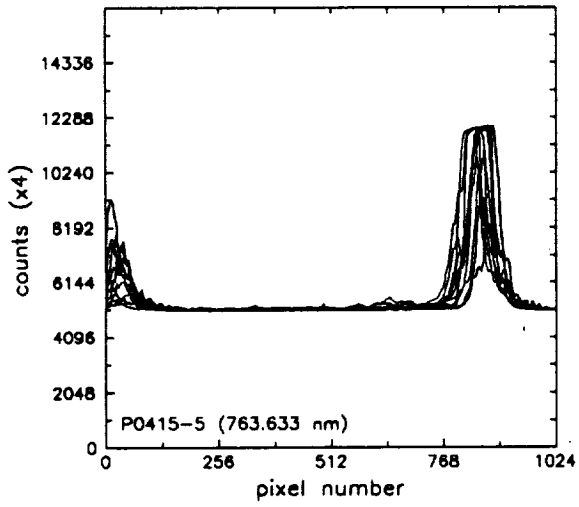

Figure 27. Superposition of 10 successive Fizeau fringes.

closely spaced in time. The variation pulse to pulse is very strong, behavior thought to be due to uncontrolled changes in the transverse mode structure. Since the pinhole aperture of the Laserscope discriminates against higher-order transverse modes, variations in the laser energy distribution among these modes will affect the energy appearing at the detector. The energy at the detector varies from a fraction of the detector range to detector saturation. Wavelength variations also appear, since the Laserscope is sampling only a portion of the laser pulse, namely the TEM00 and lowest-order transverse modes.

The broad fringe causes the Laserscope irremediable difficulties in Fizeau fringe deconvolution. The instrumental profile, the fringe produced with a good, narrow-line source, is a single fringe of the type shown (doubled due to the two longitudinal modes) in Figure 24. When this narrow fringe is subtracted from the broad fringe of Figure 25 or Figure 26, a large residue remains, and this residue is interpreted as a second laser mode. This is not truly wrong, since the laser is operating on multiple modes, but clearly the mode structure is not so simple as to be describable as the sum of two or three well-spaced modes.

The Snyder wedge was calibrated with the argon-ion laser source. This was useless for the Fizeau wedge due to the very broad laser line (4 to 6 GHz; compare the free spectral range of the Fizeau wedge, 4 GHz). The intention was to calibrate the Fizeau wedge with the pulsed dye laser. However, as might be evident from the fringes of Figure 27, this was never satisfactorily done. CAL_FIZ is the program written to perform the same least-fractions analysis which CAL_SNY executes for the Snyder wedge. The input to CAL_FIZ is a data file consisting simply of the wavelengths and the fringe peak locations (pixel numbers). This input file must be manually constructed; again, because this operation required such careful judgement, and was never very successful, automation of this procedure was not achieved. The procedure was to examine fringes carefully, such as those of Figure 26, identify the peak locations manually, and create the input file manually, including the most reliable data and excluding poor data. An example of an input file for CAL_FIZ is

```
763.6326    860
763.5192    394
764.0707    552
764.4199    397
764.5309    690
```

Figure 28 is an example of the CAL_FIZ output. As in CAL_SNY, the upper right window shows the error parameter, on a logarithmic scale, and the lower right window is an expansion of the principal minimum. A minimum is apparent, but it is quite broad. The wedge spacing corresponding to this minimum is 35.02 mm, with an uncertainty on the order of 0.05 mm, or 0.14%. Since the wedge spacing must be known to extremely high accuracy, 0.1 ppm or better, this is far from satisfactory.

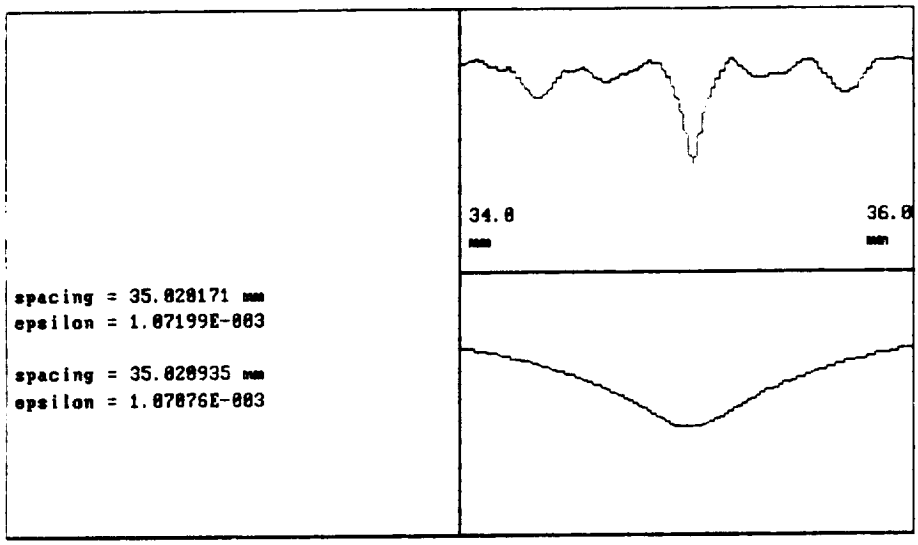

Figure 28. Video display, Fizeau wedge calibration.

The difficulties with Fizeau wedge calibration are due presumably to the source laser shortcomings, namely the pulse-to-pulse variations in fringe location. Since no better source was available, and the Laserscope development program was approaching its end, these difficulties had to be left unresolved.

If improved values of the Fizeau wedge angle or spacing are deduced, they must be inserted in HDWARE.INF manually, using an editor. Since the entries in HDWARE.INF are labelled, this is a simple operation.

The analysis of the fringe width showed that the resolution of the Fizeau wedge was as expected. In view of the calibration difficulty, as well as the problems with achieving sufficient accuracy from the Snyder wedge to determine the order number of the Fizeau interference successfully, demonstration of the potential accuracy of wavelength measurement with the wedge must be indirect.

Figure 29 shows the peak location of the fringe produced with a stabilized helium-neon laser, a source stable to parts in 10^9. The measurements were taken at intervals of 42 seconds, and the total time period of the run is 11.8 hours. The initial turn-on thermal shift, associated with opening the instrument for final alignment, is evident. The cycling of the thermostat controlling the optics temperature is also clear. After about two hours the range of variation decreases to less than 0.1 pm, peak-to-peak. The stability after six hours is about 0.05 pm, peak-to-peak.

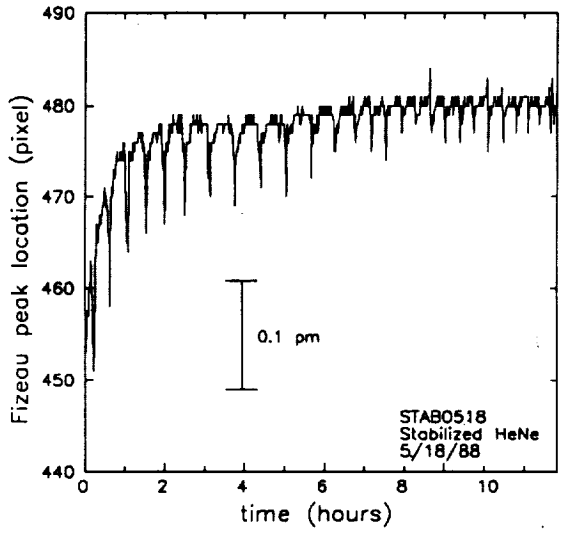

Figure 29. Fizeau fringe location vs. time, stabilized HeNe source.

Fizeau Wedge Summary

The resolution capability of the Fizeau wedge is very satisfactory, the fringes with narrow-band sources being 0.2 pm or less wide, full-width half-maximum. Thus the original goal of 0.3 pm resolution, i.e. a capability of separation of laser modes separated by 0.3 pm, has been achieved.

The stability measurements indicate that the Fizeau wedge should be capable of wavelength measurements to perhaps ±0.025 pm, the range of oscillation of the peak location due to the thermal control cycling. The actual measurement limit would depend on the ability to locate the center of the fringe with an effective width of 0.2 pm, imposed by the instrumental profile on a narrow-line source laser.

Calibration of the Fizeau wedge was an insoluble problem. The principal difficulty here is the lack of a good pulsed laser with pure TEM00 mode structure and known, variable wavelength, the pulsed analog of the argon-ion laser used for Snyder wedge calibration.

Combined Operation

The Snyder and Fizeau wedge interferometers have been considered quite separately, since their operations are almost independent, overlapping only where the Snyder wavelength calculation is used to determine the Fizeau order number.

Figure 30 is a typical instrument display. The major part of the display is the Fizeau fringe pattern, since this display can reveal a great deal of immediate information on the operation of the laser under test, including mode structure and spurious outputs. The Fizeau display is shown with a wavelength scale, 2 pm per increment. This is possible because of the linear dispersion of the Fizeau wedge. Once the order number is determined, the Fizeau scale is determined, from $\lambda(x) = 2(e_F+x\alpha)/m_F$. The wavelength scale is redrawn only if the order number changes.

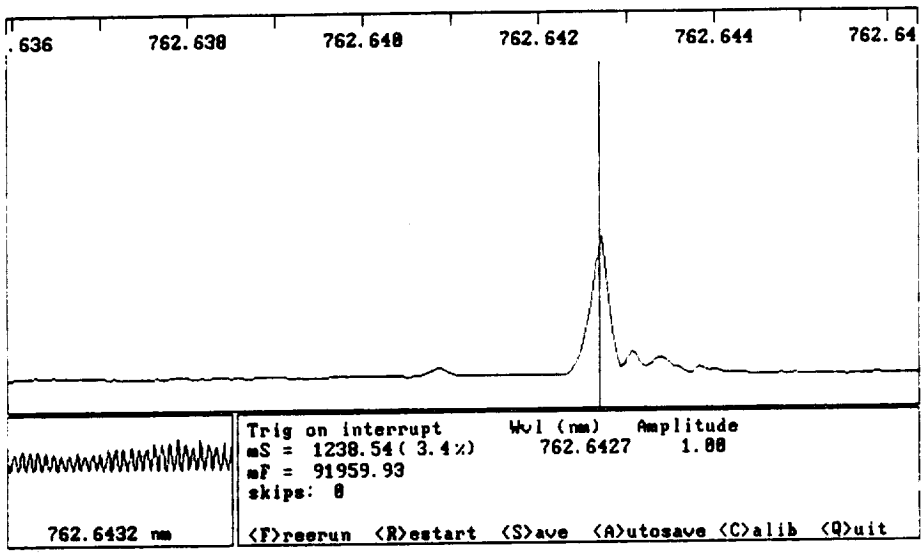

Figure 30. Laserscope operating display.

A vertical bar is drawn to indicate the center of Fizeau fringes. This will show the success of the fringe deconvolution procedure; a broad fringe, or spurious fringes, will lead to spurious fringe peak identifications, which must be ignored in the output.

The Snyder fringe display is shown in the lower-left window. This is given only a small portion of the display since it contains relatively little information that is readable directly from the raw data. It is included to permit determination of the correct amplitude and to monitor the modulation envelope.

The information panel begins with the "trigger on interrupt" or "trigger on flag" indicator. This has to do with the RC Electronics board, which is supposed to trigger on interrupts but does not always do this properly. This is useful here principally as an indicator of triggering.

The Snyder (mS) and Fizeau (mF) order numbers are displayed. The Snyder order number is particularly significant, since a value with a fractional part close to 0.5 indicates trouble. The fractional part should be with ±0.3 of the integer for reliable integer rounding. The Snyder order number is displayed with an evaluation of the scatter in node spacing (i.e., Figure 6). A scatter of a few percent is typical. Should this value become much larger than a few percent, the data will be suspect, and an inadequately clean input laser signal is indicated.

The Fizeau order number should also be close to an integer. However, in view of the insufficient accuracy of the Snyder result, this value is not very useful. As in the example shown, it is possible to have a Fizeau order number with very small fractional part, but in error by several counts.

"Skips" is a counter of laser pulses occurring before the instrument has completed processing and is ready for another pulse. This is based on the interrupt generated by the RC Electronics board, which is used to update a pulse counter and set a flag indicating that a new set of data is ready. In fact this seems not to function, for reasons never established; this issue was too minor, and the program time too short, for its resolution.

The Fizeau fringe or fringes are converted to wavelength and the peak amplitudes scaled to a sum of unity. These values are displayed to the right of the order number display. The fringe deconvolution operation is arbitrarily limited to three fringes.

Finally, a menu of options is shown. The Laserscope begins in a single-pulse mode. A keyboard input other than the specific letters shown (the space bar is appropriate) will cause it to acquire and process a single pulse. Freerun will put it into a continuous acquisition and display mode, operating at a speed determined by either its own processing speed or, for low-prf lasers, at the laser source pulse rate. Restart will allow the resetting of the program options set at the initialization of the program, for example, the frequency of Snyder fringe updates versus Fizeau fringe analyses. Save will permit data storage on a manual basis, saving selected inputs upon command. Autosave will save a sequence of inputs, the number specified at the time Autosave is invoked. Calibrate is the data storage operation prior to a Snyder wedge calibration; no automated Fizeau calibration was developed, for the reasons listed above. Quit, finally, is the exit key.

Freerun can be terminated at any time by any keyboard input. Occasionally a few pulses will pass before the machine processes the keyboard input and halts. Do not inject a repetition of keyboard inputs to stop freerunning, since the Laserscope then goes into its single-pulse mode and responds to each keyboard input stored in the keyboard buffer. Since the keyboard repetition rate is substantially higher than the data processing rate, this can force a large number of single-pulse acquisitions, simulating free-running.

Conclusion

It is clear that the Laserscope comes close to achieving the desired specifications, particularly in resolution and accuracy, but has a few critical shortcomings. The principal shortcoming is the failure of the Snyder wedge to generate reliable wavelength values outside the argon-ion calibration range. The order numbers calculated for the Fizeau wedge on the basis of the Snyder result are always unreliable, and thus the wavelengths of the Fizeau fringes computed with this order number will be unreliable. The second shortcoming is the inability to calibrate the Fizeau wedge, particularly the spacing, with good confidence. This is due entirely to the absence of a pulsed laser with the necessary single-transverse-mode operation and accurate, tunable wavelength.

A modified Laserscope, relaxing the demands on the Snyder by reducing the Snyder and Fizeau wedge spacings, would be a much more satisfactory instrument. As it is, the prototype Laserscope delivered to NASA is most suitable as a qualitative laser mode structure monitor.

References

1. J.J. Snyder, "Compact static wavemeter for both pulsed and cw lasers", Sov. J. Quantum Electron. 8, 959-960 (1978)

2. J.J. Snyder, "Apparatus and Method for Determination of Wavelength", U.S. Patent Number 4,173,442, 6 November 1979.

3. J.J. Snyder, "Algorithm for fast digital analysis of interference fringes", Appl. Opt. 19, 1223-1225 (1980).

4. James J. Snyder, "Fizeau Wavemeter", SPIE Vol. 288, Los Alamos Conference on Optics, 1981, pp. 258-262.

5. Charles K. Miller, "Wavelength meter for pulsed laser applications", Sandia Report SAND81-0310 (March 1982).

6. J.J. Snyder, "Laser Wavelength Meters", Laser Focus, May 1982, pp. 55-61.

7. J.L. Gardner, "Wave-front curvature in a Fizeau wavemeter", Opt. Lett. 8, 91-93 (1983).

8. Mark B. Morris, Thomas J. McIlrath, and James J. Snyder, "Fizeau wavemeter for pulsed laser wavelength measurement", Appl. Opt. 23, 3862-3868 (1984).

9. James L. Gardner, "Compact Fizeau wavemeter", Appl. Opt. 24, 3570-3573 (1985).

10. D.F. Gray, K.A. Smith, and F.B. Dunning, "Simple compact Fizeau wavemeter", Applied Optics 25, 1339-1343 (1986).

11. James L. Gardner, "Wavefront curvature compensation in a Fizeau wavemeter", Appl. Opt. 25, 3799-3800 (1986).

12. Lasertechnics operating manual for their Fizeau (i.e., Snyder) interferometer. Lasertechnics, Inc., 5500 Wilshire Ave. NE, Albuquerque NM 87113.

13. William S.C. Chang, Principles of Quantum Electronics, Addison-Wesley, New York, 1969.

14. P. Hariharan, Optical Interferometry, Academic Press, Orlando, Florida, 1985, pp. 119-120.

15. An excellent summary is provided in Max Born and Emil Wolf, Principles of Optics, Pergamon Press, New York (Sixth Edition, 1980), pp. 351-360.

16. G. Koppelmann, "Intensitätsverteilungen in Fizeau-Vielstrahlinterferenzen. I.", Optik 36, 474-493 (1972); "Intensitätsverteilungen in Fizeau-Vielstrahlinterferenzen. II. (Messungen bei senkrechtem Lichteinfall)", Optik 37, 164-174 (1973); and "Intensitätsverteilungen in Fizeau-Vielstrahlinterferenzen. III. (Similarity relations for oblique incidence)", Optik 40, 89-100 (1974).

17. Y.H. Meyer, "Fringe shape with an interferential wedge", J. Opt. Soc. Am. 71, 1255-1263 (1981).

18. P. Langenbeck, "Fizeau interferometer-fringe sharpening", Appl. Optics 9, 2053-2058 (1970).

NASA
National Aeronautics and Space Administration

Report Documentation Page

1. Report No.	2. Government Accession No.	3. Recipient's Catalog No.
NASA CR-181731		

4. Title and Subtitle	5. Report Date
A LASER SPECTROMETER AND WAVEMETER FOR PULSED LASERS	September 1989
	6. Performing Organization Code

7. Author(s)	8. Performing Organization Report No.
J.A. McKay, P.M. Laufer, and L.J. Cotnoir	PSI#1011/TR#800
	10. Work Unit No.
	324-02-00

9. Performing Organization Name and Address	11. Contract or Grant No.
Physical Sciences Inc. 635 Slaters Lane, Suite G101 Alexandria, VA 22314	NAS1-18243
	13. Type of Report and Period Covered
12. Sponsoring Agency Name and Address	Contractor Report
National Aeronautics and Space Administration Langley Research Center Hampton, VA 23665-5225	14. Sponsoring Agency Code

15. Supplementary Notes Langley Technical Monitor: A.L. Newcomb, Jr., Final Report - SBIR Phase II. Use of commercial products or names of manufacturers in this report does not constitute official endorsement of such products or manufacturers, either expressed or implied, by the National Aeronautics and Space Administration.

16. Abstract

The design, construction, calibration, and evaluation of a pulsed laser wavemeter and spectral analyzer are described. This instrument, called the "Laserscope" for its oscilloscope-like display of laser spectral structure, has been delivered to NASA Langley Research Center as a prototype of a laboratory instrument. The key component is a multibeam Fizeau wedge interferometer, providing high (0.2 pm) spectral resolution and a linear dispersion of spectral information, ideally suited to linear array photodiode detectors. Even operating alone, with the classic order-number ambiguity of interferometers unresolved, this optical element will provide a fast, "real-time" display of the spectral structure of a laser output.

If precise wavelength information is also desired then additional stages must be provided to obtain a wavelength measurement within the order-number uncertainty, i.e., within the free spectral range of the Fizeau wedge interferometer. A Synder (single-beam Fizeau) wedge is included to provide this initial wavelength measurement. Difficulties in achieving the required wide-spectrum calibration limit the usefulness of this function.

17. Key Words (Suggested by Author(s))	18. Distribution Statement
interferometer, wavemeter, laser	Unclassified - Unlimited Subject Category 36

19. Security Classif. (of this report)	20. Security Classif. (of this page)	21. No. of pages	22. Price
UNCLASSIFIED	UNCLASSIFIED	28	